J Mater Sci (2009) 44:204–211
DOI 10.1007/s10853-008-3100-5

Dielectric response features and oxygen migration on rare earth modified lead titanate ferroelectric ceramics

A. Peláiz-Barranco · J. D. S. Guerra · F. Calderón-Piñar · C. Aragó · O. García-Zaldívar · R. López-Noda · J. A. Gonzalo · J. A. Eiras

Received: 28 May 2008 / Accepted: 3 November 2008 / Published online: 27 November 2008

Abstract Rare earth (RE) and manganese-modified lead titanate ceramics were studied concerning the presence of two peaks in the temperature dependence of the dielectric permittivity. An eventual incorporation of the RE into A-site and/or B-site in the perovskite structure and the oxygen migration were considered as causes of the observed phenomenon. The structural analysis showed that at least a small amount of Ti^{4+} could be substituted by the RE ions. It was considered from the pyroelectric and electrical conductivity results that, even when an eventual incorporation of the RE into the A-site and/or B-site of the structure could be possible, both peaks could not be associated with paraelectric–ferroelectric (PE-FE) phase transitions. The observed peak at lower temperatures has been associated with the PE-FE phase transitions, whereas the hopping of oxygen vacancies has been considered as the cause for the dielectric anomaly observed at higher temperatures.

A. Peláiz-Barranco (✉) · F. Calderón-Piñar · O. García-Zaldívar
Facultad de Física-Instituto de Ciencia y Tecnología de Materiales, Universidad de La Habana. San Lázaro y L, Vedado, La Habana 10400, Cuba
e-mail: pelaiz@fisica.uh.cu

J. D. S. Guerra
Departamento de Física e Química, Universidade Estadual Paulista, 15385-000 Ilha Solteira, SP, Brazil

C. Aragó · J. A. Gonzalo
Departamento de Física de Materiales, Facultad de Ciencias, Universidad Autónoma de Madrid, 28049 Madrid, Spain

R. López-Noda
Departamento de Física Aplicada, ICIMAF, CITMA 15 # 551, Vedado, La Habana 10400, Cuba

J. A. Eiras
Departamento de Física, Universidade Federal de São Carlos, Rod. Wash. Luis, km. 235, 13.565-905 Sao Carlos, SP, Brazil

Introduction

Lead titanate (PT) is a potential useful ferroelectric (FE) material with a highly polar perovskite structure [1], showing a high electromechanical anisotropy in the piezoelectric response. Therefore, it becomes very attractive for many practical applications, such as surface acoustic wave devices, infrared sensors, and high frequency transducers [2, 3]. The sintering process of pure PT ceramics is very difficult because of the large tetragonality. During the cooling process, a strong crystalline anisotropy creates internal stress at the cubic-tetragonal symmetry change and the ceramics become brittle. Its fragility can be greatly reduced by the partial substitution of Pb^{2+} or Ti^{4+} ions [1]. Special attentions have been given to the rare earth (RE) ions modification, which conserves the high electromechanical anisotropy in the piezoelectric response of the sample, providing excellent materials to be used for high frequency applications [4, 5].

Previous studies carried out in RE-modified PT ceramics [6] have shown that a strong distortion of the titanium octahedron takes place after the small-radius-size ions substitution (Dy, Ho, and Er) in the lattice B-site of the perovskite structure. The substitution of Ti^{4+} (B-site) by ions showing larger ionic radius provides an increment of the tetragonality, which was observed for Er^{3+}, Ho^{3+}, and Dy^{3+}. On the other hand, two peaks were observed in the differential thermal analysis and dielectric properties of the studied ceramics. This behavior was associated with

paraelectric–ferroelectric (PE-FE) phase transitions concerning two different contributions to the total dielectric behavior of the samples, one where the RE ions occupy the A-sites, and the other where the ions occupy the B-sites of the perovskite structure [6].

Other reported results have shown dielectric anomalies in perovskite structures containing titanium [7–10], which are not related to PE-FE phase transition, but have been closely related to some conduction mechanisms. For RE doping, some authors have attributed this phenomenon to the existence of A-site vacancies in the crystalline lattice promoted by the distortion of the oxygen octahedron caused by the RE substitution [8]. On the other hand, a space-charge polarization has been also considered as the main cause for this behavior [9, 10]. As observed, PT-based FE systems present from the fundamental point of view the intriguing physical properties at high temperatures (around and above the temperature of the PE-FE phase transition), which are reflected in the dielectric response. However, there are conflicting reports concerning the existence and origin of the phase transition in these systems. Therefore, a careful investigation of the high temperature dielectric response of PT-based FE ceramics can be very interesting to contribute to the explanation for the origin of the nature of the observed anomalies. This paper presents the study carried out on $(Pb_{0.88}Ln_{0.08})(Ti_{0.98}Mn_{0.02})O_3$ FE ceramics, where Ln = La, Nd, Sm, and Gd, concerning the presence of two peaks in the temperature dependence of the real dielectric permittivity. The macroscopic effects of the eventual incorporation of the RE ions into the A-site and/or B-site of the perovskite structure are evaluated. The pyroelectric measurement results and electrical conductivity analysis suggest that the oxygen migration may be an additional cause for the obtained dielectric behavior.

Experimental procedure

Ceramic samples were prepared by the traditional ceramic method from nominal composition $(Pb_{0.88}Ln_{0.08})(Ti_{0.98}Mn_{0.02})O_3$, where Ln = La, Nd, Sm, Gd. The stoichiometric mixture of powders (PbO, TiO_2, MnO_2, Ln_2O_3) was prefired at 900 °C in air for 2 h. The calcined powders were conformed as thick disks by cold-pressing and sintered in air at 1220 °C for 2 h, in a well-covered platinum crucible. Ceramic disks of around 18 mm of diameter and 1 mm of thickness were obtained. The samples will be hereafter labeled as PT-La, PT-Nd, PT-Sm, and PT-Gd, according to the RE ions. X-ray diffraction analysis at room temperature was performed using a Rigaku Rotaflex RU200B diffractometer and CuK_α radiation. Electrodes were fabricated on the parallel faces using Au strips and an organogold paste by a heat treatment at 590 °C. The dielectric properties were measured using a HP4194A impedance analyzer in the temperature and frequency range of 27 to 550 °C and 100 Hz to 10 MHz, respectively. For the pyroelectric measurements, the samples were poled at 2 kV/mm and 80 °C for 1 h. The temperature dependence of the pyroelectric current was obtained using a Keithley 617 programmable electrometer.

Results and discussion

Dielectric behavior

Results obtained for the dielectric properties are shown in Fig. 1a and b, for the real and imaginary part of the dielectric permittivity, respectively. Figure 1a shows the temperature dependence of the real part of the dielectric permittivity (ε') at 1 kHz for the studied ceramic samples,

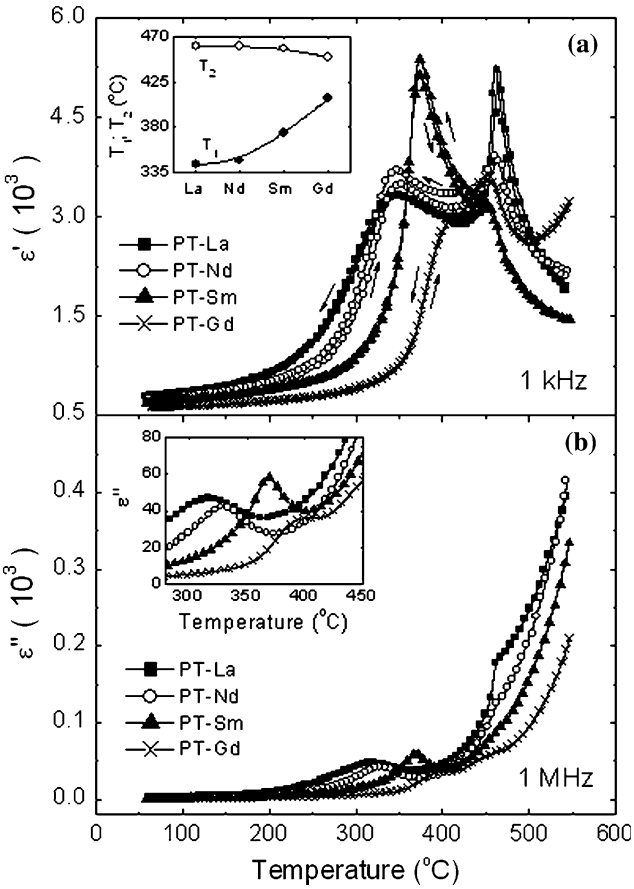

Fig. 1 **a** Temperature dependence of the real part of the dielectric permittivity (ε') at 1 kHz; the inset shows the RE ionic radii dependence of the temperature of the maximum real dielectric permittivity (T_1 and T_2, $T_1 < T_2$). **b** Temperature dependence of the imaginary part of the dielectric permittivity (ε'') for the PT-La sample, at 1 MHz

as example of the investigated behavior for the whole frequency range. The results on dielectric study have been shown for the heating and cooling stages. The presence of two peaks, which were obtained for all the analyzed frequency range, can be observed. For all the cases, the temperatures of both peaks (T_1 and T_2) did not show any frequency dependence, which is typical of 'normal' PE-FE phase transitions. Figure 1a also shows (inset Fig. 1a) the RE ionic radii dependence of the temperatures T_1 and T_2 for the studied samples. On the other hand, the 'normal' characteristic of the phase transition has been confirmed by the temperature dependence of the imaginary part of the dielectric permittivity (ε'') as a function of the frequency, not shown here, whereas no frequency dispersion of the temperature of the maximum imaginary dielectric permittivity was observed.

Figure 1b shows the temperature dependence of ε'' at 1 MHz, as example of the observed behavior for the studied materials at high frequencies region (above 500 kHz). The presence of two peaks was observed for frequencies higher than 500 kHz. In the low frequency region (below 500 kHz), only the first peak (at T_1) was observed. This result was related to the rapid increase in the imaginary part of the dielectric permittivity, which was observed for temperatures above 400 °C. With the increase of measurement frequency, the observed behavior gradually decreases, and eventually disappears in the studied temperature range for frequencies above 500 kHz, i.e., both peaks were observed.

It is well known that in perovskite FEs, oxygen vacancies could be formed during the sintering process of the samples due to the volatilization and/or charger compensation processes [11]; the electro-migration of oxygen vacancies is usually suggested as the main cause of conductivity in these materials [12]. In previous results, where the same behavior for ε'' was observed at low frequencies, the oxygen vacancy hopping processes, due to relaxations in oxygen vacancy-related dipoles, has been suggested as the main reason for the conduction behavior of perovskite FEs [12]. Thus, the rapid increase in ε'' above 400 °C for the lower frequency range (below 500 kHz) could be correlated with conductivity losses due to oxygen vacancies. On the other hand, estimated values of the electrical conductivity from ε'', between 400 and 550 °C below 500 kHz, have shown results associated with semiconductor materials [10^{-4} to 10^{-2} $(\Omega\,\mathrm{cm})^{-1}$]. A rapid increase of the conductivity values with temperature could promote an abrupt increase of ε'', which could prevent the occurence of the second peak observed in the temperature dependence of ε' above 400 °C (at T_2).

The temperature corresponding to the first peak (T_1) agrees with previous reports for these materials and is associated with the PE-FE phase transition [13, 14]. It is important to point out, by direct inspection of Fig. 1a, the presence of a slight thermal hysteresis-like behavior for temperatures around T_1, characterized by a small difference between the temperatures of the heating (T_{1h}) and the cooling (T_{1c}) stages. This behavior has been extensively studied in the literature, and it has been associated with intrinsic mechanisms related to the structural and elastic properties of the FE materials [15]. In this way, an observed difference between the Curie temperature (T_C) on heating and the T_C on cooling, referred to as "thermal hysteresis" of the PE-FE phase transition, as previously observed in $BaTiO_3$, has shown to be a consequence of several factors, such as impurities, grain sizes, and defects, promoted by the doping amount added to the above-mentioned system [16]. The Curie temperature on heating is always larger than that observed on cooling stage. Consequently, the thermal hysteresis is found to be strongly dependent on the grain size of the FE materials [17]. The influence of these factors on the observed dielectric anomalies has been extensively investigated in the last years in materials not only in ceramic form, but also as single crystals. As for explaining and modeling the effect of such factors in the thermal hysteresis, several hypotheses have been proposed. Therefore, the occurrence of such common thermal hysteresis in ceramics and/or single crystal FE systems, and its dependence with the previously mentioned factors, has encouraged the development of several mutually excluding explanations and models to explain this physical phenomenon [17–19]. However, it can be seen from the current literature that this topic has not yet been clarified.

The usual, and most accepted, method for a theoretical description of the PE-FE phase transition is the one provided by the Landau-Devonshire theory [20], which was first used for modeling the phase transitions in FE single crystals, and has been validated nowadays for ceramics. According to this theory, FEs undergoing a first-order phase transition are characterized by a set of temperatures limiting the meta-stable regions of both FE and PE phases in such a way that the first-order PE-FE phase transition proceeds in a domain of temperatures and not at a fixed temperature, as in the case of the second-order phase transition.

However, a direct inspection of the differences between T_{1h} and T_{1c} for all the studied samples (see Table 1) shows smaller values for the thermal hysteresis than those observed for some other classical FE systems, which are found to be around 10–15 °C, as reported in the literature [16]. As observed, with the increase of the ionic radius the thermal hysteresis clearly decreases, which shows clear evidences that the observed behavior becomes largely dependent on the intrinsic factors associated with structural and elastic characteristics, related to the doping element.

Table 1 Thermal hysteresis, structural parameters, and activation energy values associated with the dc conductivity for the studied ceramic samples

Samples	$T_{1h} - T_{1c}$ (°C)	E_a (eV)	c (Å)	a (Å)	c/a
PT-La	3.8	0.90 ± 0.05	4.041	3.910	1.03
PT-Nd	2.4	0.94 ± 0.05	4.056	3.905	1.04
PT-Sm	0.8	0.96 ± 0.05	4.091	3.899	1.05
PT-Gd	–	1.09 ± 0.05	4.125	3.894	1.06

Such dependence of the differences between PE and FE states with the RE ion implies that internal stress can be directly affected by the increase of the ionic radii of the RE ions, since internal stresses do not grow in the cubic phase but develop when samples are cooled below T_C. This result may be an indication that the nature of the PE-FE phase transition in the studied samples could be related to a second-order [21] rather than a first-order phase transition. In order to better clarify this issue, the dielectric properties have now been investigated by the analysis of the temperature dependence of $1/\varepsilon'$ for all the studied samples. In this way, the slope of data for temperatures below and above T_1 has been determined taking into account a linear fitting, as shown in Fig. 2 for the PT-La and PT-Nd samples, as representative curves. Results revealed that the slopes of the curves below T_1 are about twice higher than those obtained for temperatures above T_1, being 2.2 and 2.1 for the PT-La and PT-Nd samples, respectively. This obtained result, which is typical of second-order phase transitions [21], shows strong evidences that the nature of the PE-FE phase transition for the studied samples corresponds to a true second-order phase transition, in agreement with previous results reported for pure PT materials [22].

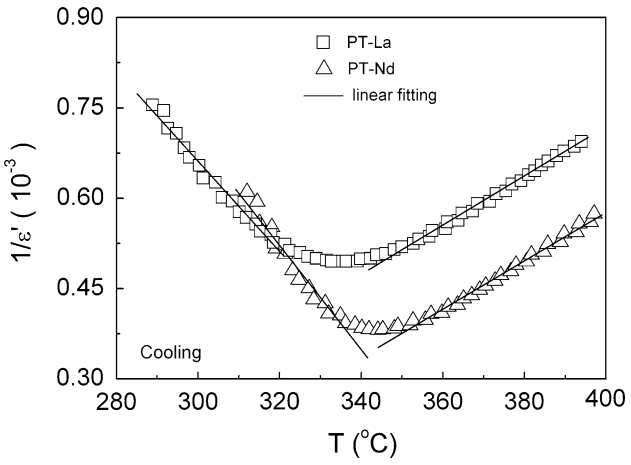

Fig. 2 Temperature dependence of $1/\varepsilon'$ for temperatures below and above T_1 (on cooling stage), for the PT-La and PT-Nd samples, at 1 kHz

By considering that T_1 has been associated with the PE-FE phase transition, the first intriguing question is, what is the phenomenon associated with the higher temperature second peak, related to T_2. Usually, the temperature dependence of ε' for FE materials show peaks associated with PE-FE as FE-FE phase transitions, similar to the successive obtained phase transitions in the $BaTiO_3$ [22]. Taking into account the observed behavior for the studied samples, results can be discussed concerning the previously observed phenomenon for the REs-modified PT ceramics with Dy, Ho, and Er in the B-site [6]. Considering this analysis, at least a small amount of Ti^{4+} could be substituted by the REs. Thus, the obtained peak observed around T_1 and T_2 could be associated with different contributions, taking into account the occupation ratios of A- and B-sites, respectively, by the RE ions. The question is whether an eventual incorporation of the REs ions in the B-sites considering their high ionic radii could be possible.

Structural analysis

Figure 3 shows the X-ray diffraction patterns at room temperature for the studied samples. Results on structural analysis of the studied ceramic compositions revealed pure tetragonal perovskite structures for all the cases. Results on the variation of lattice parameters (c, a) and the tetragonality (c/a) with the RE ionic radius, obtained from the structural analysis, are shown in Table 1. As can be observed, the tetragonality increases as the RE ionic radius decreases.

On the other hand, considering the nominal composition, it should be analyzed for two modification types concerning the pure PT system. Table 2 shows the ionic

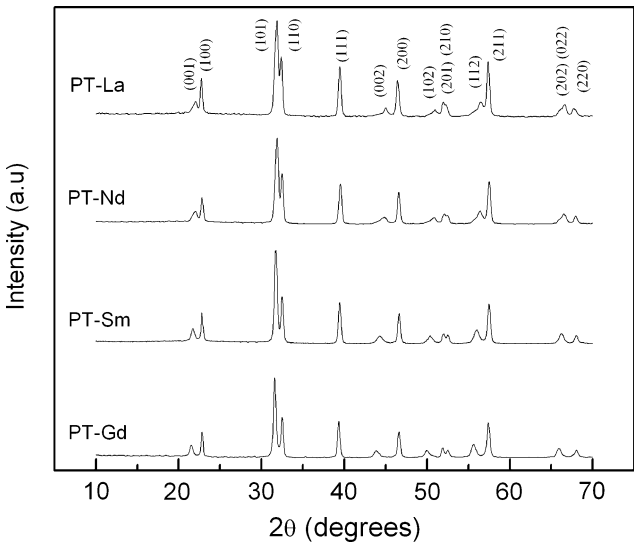

Fig. 3 X-ray diffraction patterns at room temperature for the studied samples

Table 2 Ionic radius corresponding to hexa- and dodeca-coordinated sites

Ions	Ionic radii (Å)	
	Hexa-coordinated site	Dodeca-coordinated site
Pb^{2+}	–	1.63
Ti^{4+}	0.74	–
Mn^{4+}	0.67	–
La^{3+}	1.17	1.50
Nd^{3+}	1.12	1.41
Sm^{3+}	1.09	1.38
Gd^{3+}	1.08	–

radius and coordination numbers of the hexa- and dodeca-coordinated site elements, obtained from the previously reported results in reference [23]. The partial substitution of Ti^{4+} (B site, hexa-coordinated site) by small amounts of manganese ions provides a lower tetragonality when compared to that for the pure PT system [4, 22]. For the REs substitutions, three possible situations should be considered. The first one is the substitution of Pb^{2+} (A-site, dodeca-coordinate site) by small amounts of RE ions, which should provide a decrement of the tetragonality. The second one is the substitution of Ti^{4+} by small amounts of RE ions, which should provide an increment of the tetragonality. The last one is the substitution in both A- and B-sites, which could provide either an increment or a decrement of the tetragonality. Therefore, the tetragonality results observed in Table 1 suggest that at least a small amount of Ti^{4+} could be substituted by the REs. For instance, in the present case, the RE could occupy both A- and B-sites of the perovskite structure.

It can be noted that the ceramic samples have been prepared considering vacancies in A-site. In general, it could be written as $(Pb_{1-3x/2}Ln_xV_{x/2})(Ti_{0.98}Mn_{0.02})O_3$, where $x = 0.08$ and V means vacancies. However, previous results have shown that at least the small-radius-size substitution (Dy, Ho, and Er) could occupy the B-sites of the perovskite structure [6]. Thus, it could be interesting to evaluate the possibility of an eventual incorporation of any amount of RE ion in the A-site and/or B-site. Taking into account that the RE ions could now occupy any site, the formula $(Pb_{1-3x'/2+y}Ln_{x'}V_{x'/2})(Ti_{0.98}Mn_{0.02}Ln_y)O_{3+5y/2}V\ddot{o}_{y/2}$ can be obtained. As can be seen, in this new expression $x' + y = 0.08$, because in the new analysis the initial nominal composition has been considered (i.e., the ceramic samples have been prepared considering an 8 at.% RE).

From this new expression, the stability of the perovskite structure was evaluated considering an eventual incorporation of some part of REs in the B-sites. This analysis was carried out taking into account the tolerance factor values in the range of $0.77 \leq t \leq 1$ for a stable perovskite structure [24]. Figure 4 shows the tolerance factor values as a function of y (possible concentration of REs in the B-sites). The analysis was carried out considering the change in the y values from 0 to 0.08, which shows several situations [(i) $y = 0$, the REs could occupy only A-sites; (ii) $0 < y < 0.08$, the REs could occupy both A- and B-sites; (iii) $y = 0.08$, the REs could occupy only B-sites). Figure 4 shows only the y-range values for a stable perovskite structure. As can be seen, some part of the RE ions (below the fourth part of the 8 at.% RE) could occupy the B-sites, providing a stable perovskite structure.

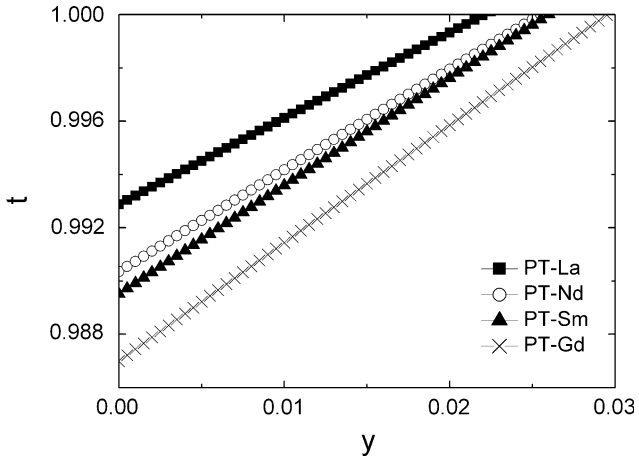

Fig. 4 Tolerance factor values considering an eventual incorporation of small concentration of REs ions in the B-sites (y)

From these results, it could be concluded that an eventual incorporation of the REs into B-sites of the perovskite structure could be possible. Thus, the above-mentioned discussion suggests that obtained dielectric results could be associated with the two different A- and B-sites occupation situations, one where the RE ions occupy the A-sites and other one where they occupy the B-sites of the structure.

Pyroelectric behavior and oxygen migration

The RE-modified PTs are known as donor doped ceramics, which show a conduction mechanism due to a low concentration of oxygen vacancies [24]. This analysis can be carried out considering the incorporation of the RE ions into the A-site of the perovskite structure, providing lead vacancies in order to compensate the charge imbalance. If an eventual incorporation of the REs into the B-sites of the perovskite structure is possible to occur, oxygen vacancies have to be created to compensate for the charge imbalance [22]. Therefore, the oxygen vacancies concentration in the studied samples might have an important contribution in the obtained dielectric response. On the other hand, electronic paramagnetic resonance investigations carried out in the studied ceramic system have shown a valence change from 4+ to 2+ in the Mn ion during the sintering process

[25]. As a consequence, oxygen vacancies have to be created in order to compensate for the charge imbalance.

Computational simulations of the ionic transport in perovskite oxides [26] indicate that the activation energy for the oxygen migration is around 1 eV. On the other hand, the activation energies for the A- and B-sites cation transport are around 4 and 12 eV, respectively. Thus, oxygen ions are known to show a certain motion in perovskite ceramics [26, 27]. Figure 5 shows the temperature dependence of the pyroelectric current (i_p) for the PT-Nd, which has been selected as the representative curve. Similar behavior was obtained for all the other samples. The pyroelectric effect, whereby a change in temperature in a material engenders a release of electric charge, has been known as a physically observable phenomenon for many years [28]. From the microscopic viewpoint, the pyroelectric effect occurs because of the asymmetric environment experienced by electrically charged species within the crystal structure of the material. In this way, the ions within the crystalline lattice are displaced relative to the unit cells (charges center) to give rise to an electrical dipole moment (or spontaneous polarization) along the displacement direction. The electrical dipole is created by the charge of the cations located at the unit cell of the crystalline lattice and the surrounding oxygen elements. Thus, positive and negative charges centers, placed asymmetrically, constitute the FE dipole. Any excitation caused by an increase in lattice temperature (thermal fluctuations) will change its quantized energy level and, consequently, leads to a change in its mean equilibrium position in the lattice along the displacement direction. This gives a change in the overall electrical dipole moment, which appears as the macroscopic pyroelectric effect. Therefore, the pyroelectric effect manifests itself as a release of charge at the surface of the material when its temperature is changed. These changes can be detected as a current (i_p), frequently termed as pyroelectric current, flowing in an external circuit. In most of cases the largest pyroelectric effects are observed in FE materials [29, 30], in which the direction of the dipole moment can be switched by the application of an electric field. In these materials, the polar low symmetry pyroelectric phase is related to a higher symmetry phase by means of a reversible structural displacement occurring at a transition temperature, known as the Curie temperature (T_C) [20].

Usually, the high temperature structure is non-polar (termed as PE phase) and thus the spontaneous polarization tends to decrease with the increase of the temperature, tending to zero at T_C. Hence, with the increase of the temperature the pyroelectric current shows a maximum for temperatures below T_C, and tends to zero at the Curie temperature. Thus, as can be seen in Fig. 6 for the studied samples, the pyroelectric current vanishes at T_1, indicating that the polarization of the system disappears at this temperature. Therefore, this temperature can be associated with the temperature of the PE-FE phase transition (where the polarization disappears), in correspondence with the observed results for the real and imaginary dielectric permittivity (Fig. 1a, b).

On the other hand, for temperatures higher than T_1, the i_p shows negative values, which in turn continuously decrease reaching very large negative values, even above T_2. The pyroelectric current data for temperatures above 400 °C have not been shown in Fig. 5, because of the high negative magnitude values obtained for i_p, which might mask the scale for the pyroelectric peak in the FE phase. This anomalous behavior, obtained during heating of poled FE samples, has been previously associated with additional

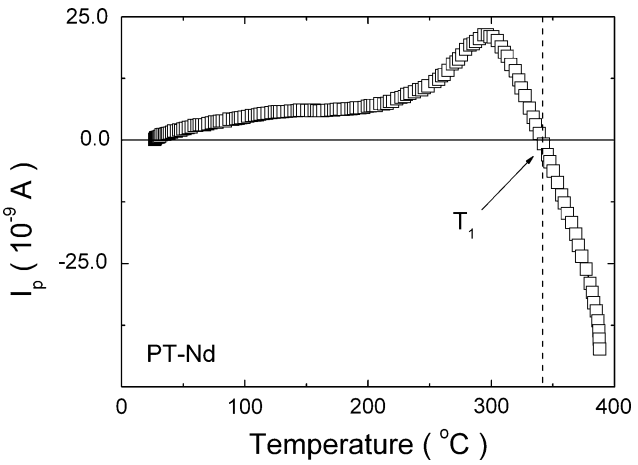

Fig. 5 Temperature dependence of the pyroelectric current (i_p) for the PT-Nd sample

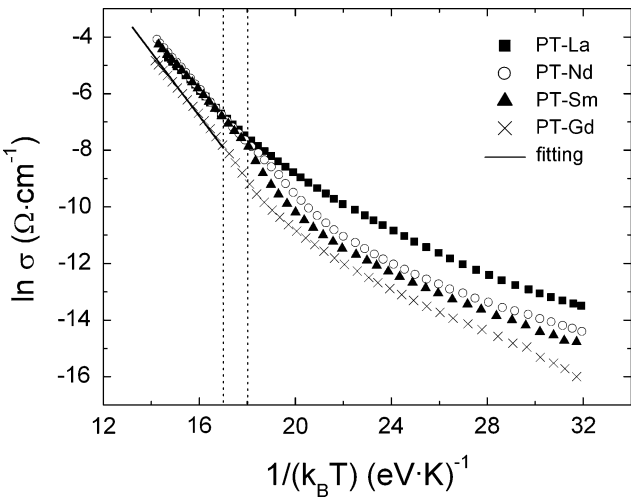

Fig. 6 Temperature dependence of the electrical conductivity at 1 kHz. The region between the *dashed lines* shows the temperature region where the first peak (T_1) appears

dielectric absorption effects, which mask the real pyroelectric effect and are commonly observed for temperatures higher that the PE-FE phase transition temperature (T_C) [31]. Indeed, at temperatures above the Curie point, additional discharges of very substantial magnitude occur [31, 32], far exceeding the actual FE polarization, leading to extremely large negative values of the pyroelectric current. This anomalous polarization, which has not been associated with the ferroelectricity phenomenon, has been explained as the release of energy stored in a form of secondary cell activity involving oxygen vacancies [33], which act as charge carriers and interact with the metal electrodes. Thus, the anomalous effect frequently observed in the temperature dependence of the pyroelectric current for some FE materials can be ascribed to electrolytic activity involving oxygen vacancies. Therefore, considering the observed results in Fig. 5, the obtained behavior for i_p at temperatures above T_1 could be associated with the oxygen motions by a vacancy mechanism, which has been in turn supported by previous studies in perovskite structure-type systems [31, 32].

In order to evaluate the oxygen migration by a vacancies mechanism, the electrical conductivity (σ) has been obtained from the imaginary part of the dielectric permittivity. Figure 6 shows the temperature dependence of the electrical conductivity for the studied samples at 1 kHz, as an example of the behavior observed for the analyzed frequency range. For temperatures higher than T_1 a linear behavior is identified as dc conductivity component (σ_{dc}). It can be noted that the temperature region between the dashed lines denotes the temperature region where the first peak (T_1) appears. From the fitting of the experimental data taking into account an Arrhenius-type dependence, which has been shown in Fig. 6 for the PT-Gd sample, the corresponding activation energy values were obtained (see Table 1). The results confirm that above T_1 the conduction process can be associated with oxygen migration, as reported in the literature [27, 32, 33] and previously discussed in the pyroelectric response results. Thus, from the pyroelectric analysis and the electrical conductivity behavior it can be concluded that the observed peak around T_1 and the anomalous behavior for temperatures higher than T_1, in the dielectric response, can be associated with the PE-FE phase transition and an oxygen migration by a vacancies mechanism, respectively.

Therefore, even when an eventual incorporation of the RE into the A-site and/or B-site of the perovskite structure could be possible, the peaks observed in the temperature dependence of the real dielectric permittivity could not be associated with the existence of two PE-FE phase transitions. In fact, the first one (observed at T_1) can be associated with the PE-FE phase transition. Above T_1 there is a significant contribution of the oxygen vacancies to the dielectric response. The oxygen vacancies hopping mechanism, which is similar to the reorientation of the FE dipoles, leads to the dielectric anomaly observed at T_2.

Conclusions

A detailed investigation of the dielectric and electric properties has been carried out on $(Pb_{0.88}Ln_{0.08})(Ti_{0.98}Mn_{0.02})O_3$ FE ceramics (where Ln = La, Nd, Sm, and Gd), in order to evaluate the macroscopic effects of the eventual incorporation of the REs into the A-site and/or B-site of the perovskite structure and the oxygen migration processes. Two peaks were observed in the temperature dependence of the real dielectric permittivity, for all the studied frequency range. The pyroelectric analysis showed that the spontaneous polarization of the FE system disappears at the temperature corresponding to the first peak (T_1), which has been in turn considered to be related to the PE-FE phase transition temperature. On the other hand, the electrical conductivity behavior confirmed that the observed anomalies for temperatures above T_1 can be associated with an oxygen migration by a vacancies mechanism, as previously revealed by the pyroelectric response features in the PE region.

Acknowledgements The authors wish to thank the Third World Academy of Sciences (RG/PHYS/LA No. 99-050, No. 02-225, No. 05-043) and FAPESP Brazilian agency (Proc. No. 06/60013-5) for financial support, and ICTP for financial support of Latin-American Network of Ferroelectric Materials (NET-43). Dr. Peláiz-Barranco wishes to thank Universidad Autónoma de Madrid for financial support. Dr. Calderón-Piñar wishes to thank the ICTP program for Training and Research in Italian laboratories.

References

1. Rossetti GA, Cross LE, Cline JP (1999) J Mater Sci 30:24. doi: 10.1007/BF00352127
2. Ito Y, Takeuchi H, Nagatsuma N, Jyomura S, Ashida S (1981) J Appl Phys 52:3223
3. Ichinose N (1985) Am Ceram Soc Bull 64:1581
4. Pérez-Martínez O, Calderón F, Pentón A, Suaste E, Rivera M, Leccabue F, Boccelli G, Watts E (1995) Rev Mex Fis 41:85
5. Pérez-Martínez O, Saniger JM, Peláiz-Barranco A, Calderón-Piñar F (1999) J Mater Res 14:3083
6. Pérez-Martínez O, Saniger JM, Torres-García E, Flores JO, Calderón-Piñar F, Llópiz JC, Peláiz-Barranco A (1997) J Mat Sci Lett 16:1161
7. Ch Ang, Yu Z, Cross LE (2000) Phys Rev B 62:228
8. Johnson DW, Cross LE, Hummel FA (1970) J Appl Phys 41:2828
9. Stumpe R, Wagner D, Bauerle D (1983) Phys Stat Sol A 75:143
10. Bidault O, Goux P, Kchikech M, Belkaomi M, Maglione M (1994) Phys Rev B 49:7868
11. Kang BS, Choi SK, Park CH (2003) J Appl Phys 94:1904
12. Peláiz-Barranco A, Guerra JDS, López-Noda R, Araújo EB (2008) J Phys D Appl Phys 41:215503

13. Takeuchi H, Jhomura S, Nakaya P, Ishikawa Y (1983) Jpn J Appl Phys 22:166
14. Takeuchi H, Jhomura S, Nakaya P (1985) Jpn J Appl Phys 24:36
15. Tura V, Mitoseriu L, Papusoi C, Osaka T, Okuyama M (1998) J Electroceram 2:163
16. Kinoshita K, Yamaji A (1976) J Appl Phys 47:371
17. Frey MH, Payne DA (1996) Phys Rev B 54:3158
18. Arlt G (1990) J Mater Sci 25:2655. doi:10.1007/BF00584864
19. Zhong WL, Wang YG, Zhang PL (1994) Phys Lett A 189:121
20. Lines ME, Glass AM (1977) Principles and applications of ferroelectrics and related materials. Clarendon Press, Oxford
21. Strukov BA, Levanyuk AP (1998) Ferroelectric phenomena in crystal. Springer-Verlag, Berlin
22. Xu Y (1991) Ferroelectric materials and their applications. Elsevier Science Publishers, Netherlands
23. Cotton FA, Wilkinson G, Wilkinson CA, Bochmann M (1999) Advanced inorganic chemistry. Wiley, New York
24. Halliyal A (1987) Am Ceram Soc Bull 66:671
25. Ramírez-Rosales D, Zamorano-Ulloa R, Pérez-Martínez O (2001) Solid State Comm 118:371
26. Saiful-Islam M (2000) J Mater Chem 10:1027
27. Jiménez B, Vicente JM (1998) J Phys D Appl Phys 31:446
28. Lang SB (1974) Ferroelectrics 7:231
29. Berlincourt D (1956) IRE Trans Ultrason Eng 4:53
30. Jaffe H (1958) J Am Ceram Soc 41:494
31. Berlincourt D, Crolik C, Jaffe H (1960) Proc IRE 48:220
32. Blood HL, Levine S, Roberts NH (1956) J Appl Phys 27:660
33. Northrip JW (1960) J Appl Phys 31:2293